TWMS J. App. Eng. Math. V.9, N.3, 2019, pp. 525-534

BLIND DECONVOLUTION USING SHEARLET -TV REGULARIZATION

Z. MOUSAVI[1], R. MOKHTARI[1], M. LAKESTANI[2], §

Abstract. In this article we propose two minimization models for blind deconvolution. In the first model, we use shearlet transform as a regularization term for recovering image. Also total variation method is used as a regularization term for point spread function(PSF). To speed up the process, Fast ADMM approach is exploited. In the second model, shearlet transform is utilized as a regularization term for both image and PSF.

Keywords: shearlet, total variation, blind deconvolution, Fast ADMM, Image processing.

AMS Subject Classification: 94A08, 97N40, 68U10.

1. Introduction

The goal of image deblurring is to estimate an image with the high quality, which has been degraded by camera motion, also the noise resulted from the imaging devices. When the degradations can be modeled as a convolution operation, the act of restoring the original image from the degraded blurred image, frequently called deconvolution [1]. We denote the model of degradated image as

$$h \otimes f + n, \tag{1}$$

where h is a convolution kernel or point spread function (PSF) of the imaging system, f is the original image and n is Gaussian white noise . Recovering f and h using only the degraded image g is called blind deconvolution [2]. Several methods presented the recovering of the deblurred image and PSF in (1) simultaneously. Nakagi et al. [3] presented a VQ-based blind image restoration algorithm. Panchapakesan et al. [4] introduced a blur identification method from vector quantizer encoder distortion. The authors of [5, 6, 7] used inverse filtering methods and Cannon used a Tikhonov regularization[9]. Liao et al. used a GCV approach [13]. We refer to [2, 11-16, 21-25] and references therein, for more informations in blind deconvolution.

Blind image deconvolution is an ill-posed problem [13], hence You and Kaveh designed in [20] a regularizing approach to join blur identification and image restoration. They considered

[1] Department of Mathematical Sciences, Isfahan University of Technology, Isfahan 84156-83111, Iran.
e-mail: zr.mousavi@gmail.com; ORCID: https://orcid.org/0000-0002-2240-4837.
e-mail: mokhtari@cc.iut.ac.ir; ORCID: https://orcid.org/0000-0002-1420-0949.
[2] Faculty of Mathematical sciences, University of Tabriz, Tabriz, Iran.
e-mail: lakestani@tabrizu.ac.ir; ORCID: https://orcid.org/0000-0002-2752-0167.
§ Manuscript received: May 23, 2017; accepted: October 9, 2017.
TWMS Journal of Applied and Engineering Mathematics, Vol.9, No.3 © Işık University, Department of Mathematics, 2019; all rights reserved.

the following problem:

$$\min_{f,h}\|f \otimes h - g\|_2^2 + \lambda_1\|Df\|_2^2 + \lambda_2\|Dh\|_2^2, \tag{2}$$

where D is the first-order differencing matrix, λ_1 and λ_2 are the two positive regularization parameters which weigh their contribution. Also Chan and Wong [21] investigated the following blind deconvolution problem:

$$\min_{f,h}\|f \otimes h - g\|_2^2 + \lambda_1 TV(f) + \lambda_2 TV(h). \tag{3}$$

The definition of discrete TV norm will be given in section IV. Total variation regularization model (3) has superior performance when applied to piecewise constant images but it becomes less effective when images contain complex textures and edges.

The multiscale and multidirectional features of the shearlet transform provide a good estimation ability for restoring images which are more complicated.

According to this point, in this article, we consider two blind deconvolution models. In the first model, shearlet transform is employed as a regularization term for recovering f (original image) and the total variation regularization is used for restoring h. In the second model shearlet transform is used for concurrent restoring f and h (point spread function) from the observation image g.

Alternating direction method of multipliers (ADMM) is a common tool for solving minimization problems. ADMM with a predictor-corrector-type acceleration stage results to accelerated variant of ADMM to solve minimization problem. This method is called Fast ADMM [27]. Here we solve minimization problems using the ADMM and Fast ADMM methods.

The rest of the paper is structured as follows. In Section 2, the shearlet transform and its implementation are described. We solve a deconvolution minimization problem using Fast ADMM method in section 3. In section 4, we present two blind deconvolution models. Experimental results are presented in section 5, and finally we conclude the paper in section 6.

2. Shearlet Transform

The shearlet transform is a directional representation system based on anisotropic dilation which is able to describe geometry of multidimensional functions [28]. Let $\psi \in L^2(\mathbb{R}^2)$ and

$$A_a = \begin{pmatrix} a & 0 \\ 0 & \sqrt{a} \end{pmatrix}, \quad B_s = \begin{pmatrix} 1 & s \\ 0 & 1 \end{pmatrix},$$

where A_a is an anisotropic dilation matrix and B_s is a shear matrix. The Continuous Shearlet System $SH(\psi)$ is defined by

$$SH(\psi) = \{\psi_{a,s,t}(x) = a^{-3/4}\psi(A_a^{-1}B_s^{-1}(x-t)) : a > 0, s \in \mathbb{R}, t \in \mathbb{R}^2\}. \tag{4}$$

The continuous shearlet transform of a function $f \in L^2(\mathbb{R}^2)$ is given by

$$f \in L^2(\mathbb{R}^2) \longrightarrow SH_\psi(f)(a,s,t) =< f, \psi_{a,s,t} > . \tag{5}$$

However, disadvantage of defined shearlet system is bias toward certain axis. This problem is circumvented by definition cone-adapted discrete shearlet system. Furthermore, all the bandwise discrete shearlet transforms can be computed effectively by employment the discrete Fourier transform and the discrete inverse Fourier transform . Let $SH_i(f)$ represents the discrete shearlet transform of f that is ith subband of the shearlet transform. Moreover, suppose H_1 is the fast Fourier transform or FFT of the discrete 2D scaling function, and $H_i\,(i \geq 2)$ are those of the discrete shearlets [29].

In this paper we employ band limited shearlets (with compact supports in the Fourier domain) [30], which is effortless to derive the inversion as a tight frame.

3. Deconvolution by Fast ADMM method

In this section, we formulate the deconvolution problem as follows:

$$\min_f \frac{\mu}{2}\|f \otimes h - g\|_2^2 + \lambda \sum_{i=1}^{N} \|SH_i(f)\|_1, \tag{6}$$

where $SH_i(f)$ is the ith subband of the shearlet transform of f. Introducing auxiliary variables $w_i, (i = 1, ..., N)$, (6) is equivalent to

$$\min_{f,w_i} \frac{\mu}{2}\|f \otimes h - g\|_2^2 + \lambda \sum_{i=1}^{N} \|w_i\|_1, \tag{7}$$

$$SH_i(f) = w_i \quad i = 1, 2, ..., N. \tag{8}$$

Introducing the dual variable $P = \{p_i\}_{i=1}^N$, and applying Fast ADMM for solving (7), we get the following algorithm:

Algorithm 1: Fast ADMM for deconvolution

Input: convolution operator h, observed image $g, \beta_1 = 1, P = 0$.

for $k = 1, 2, 3, ...$ **do**

1. $w_i^k = \arg\min_{w_i} \ \|w_i\|_1 + \frac{\alpha_1}{2}\|w_i - SH_i(f) + p_i^k\|_2^2, \ \ i = 1, 2, ..., N,$
2. $\bar{f}^k = \arg\min_{\bar{f}} \ \frac{\mu}{2}\|\bar{f} \otimes h - g\|_2^2 + \frac{\lambda\alpha_1}{2}\sum_{i=1}^{N}\|SH_i(\bar{f}) - w_i^k - p_i^k\|_2^2,$
3. $\bar{p}_i^{k+1} = p_i^k + \gamma(SH_i(\bar{f}^k) - w_i^k), \quad i = 1, 2, \ldots, N,$
4. $\beta^{k+1} = \dfrac{(1 + \sqrt{1 + 4(\beta^k)^2})}{2},$
5. $f^{k+1} = \bar{f}^k + \dfrac{\beta^k - 1}{\beta^{k+1}}(\bar{f}^k - \bar{f}^{k-1}),$
6. ${p_i}^{k+1} = \bar{p}_i^k + \dfrac{\beta^k - 1}{\beta^{k+1}}(\bar{p}_i^{k+1} - \bar{p}_i^k), \quad i = 1, 2, \ldots, N,$
7. $\lambda = \lambda * .98,$

end

In step 1, the explicit formulas for w_i^k is:

$$w_i = \text{shrink}(SH_i(f) + p_i, 1/\alpha_1), i = 1, ..., N,$$

where $\text{shrink}(a, b) = \text{sgn}(a). * \max(|a| - b, 0)$.

In step 2, to solve the $\bar{f}$-subproblem, we have $SH_i(\bar{f}) = H_i. * \text{fft2}(\bar{f})$, therefore:

$$\bar{f} = \text{ifft2}\left(\frac{\mu * \text{conj}(\text{fft2}(h)). * \text{fft2}(g) + \alpha_1\lambda\sum_{i=1}^{N}(H_i. * \text{fft2}(w_i - p_i))}{\sum_{i=1}^{N}\alpha_1\lambda(H_i. * H_i) + \mu * \text{conj}(\text{fft2}(h)). * \text{fft2}(h)}\right),$$

where fft2 is 2-D Fourier transform and ifft2 is inverse 2-D Fourier transform.

Fast alternative direction method is used in process solving proposed model for restoring original image in next section.

4. Proposed Algorithms

In this section, we present two models for blind deconvolution problem.

A. Blind deconvolution by SH-TV regularization

In the first form, we apply shearlet transform as a regularization term of an image and use the total variation method as regularization term of PSF. This can be written as:

$$\min_{f,h} \quad \frac{\mu}{2}\|f \otimes h - g\|_2^2 + \lambda_1\|h\|_{TV} + \lambda_2 \sum_{i=1}^{N} \|SH_i(f)\|_1, \tag{9}$$

where $SH_i(f)$ is the ith subband of the shearlet transform of f. The TV-norm, $\|h\|_{TV}$, can either be the anisotropic TV norm :

$$\|h\|_{TV} = \sum_i |(D_x h)_i| + |(D_y h)_i|, \tag{10}$$

or the isotropic TV norm :

$$\|h\|_{TV} = \sum_i \sqrt{(D_x h)_i^2 + (D_y h)_i^2}, \tag{11}$$

where $D_x h = \mathbf{vec}(h(x+1,y) - h(x,y)), D_y h = \mathbf{vec}(h(x,y+1) - h(x,y))$. Here we apply anisotropic TV norm. The isotropic TV, can be similarly derived.

Without using a priori information, let initial f be the observed image and initial h be the delta function in our numerical results. Iterative procedure for solving the problem (9) is formulated in Algorithm 2 :

Algorithm 2

Input: an initial image f, an initial PSF h and an observed image g

for $k = 1, 2, 3, ...$ **do**

1. Solve for h^k :

$$h^k = \arg\min_h \ \frac{\mu}{2}\|f^{k-1} \otimes h - g\|_2^2 + \lambda_1 \|h\|_{TV}, \tag{12}$$

2. Solve for f^k :

$$f^k = \arg\min_f \ \frac{\mu}{2}\|f \otimes h^k - g\|_2^2 + \lambda_2 \sum_{i=1}^{N} \|SH_i(f)\|_1. \tag{13}$$

end

a. h-Subproblem: The minimization problem (9) may not have a unique solution. For obtaining an acceptable solution, natural and physical conditions on f and h can be imposed as what follows [21],

$$h \geq 0, \ \sum_{i,j} h_{i,j} = 1, \quad f \geq 0. \tag{14}$$

Let $D = (D_x, D_y)$, therefore $\|h\|_{TV} = \|Dh\|_1$ and hence the minimization problem (12) can be rewritten as:

$$\min_h \ \frac{\mu}{2}\|f \otimes h - g\|_2^2 + \lambda_1 \|Dh\|_1, \tag{15}$$

which is equivalent to:

$$\min_{h,z} \ \frac{\mu}{2}\|f \otimes h - g\|_2^2 + \lambda_1 \|z\|_1, \tag{16}$$

$$s.t \ \ z = Dh. \tag{17}$$

Introducing the dual variable y, the augmented Lagrangian can be written as

$$h = \arg\min_{z,h} \|z\|_1 + \frac{\mu}{2\lambda_1}\|f \otimes h - g\|_2^2 + < y, z - Dh > + \eta_r \|Dh - z\|_2^2. \tag{18}$$

For the estimating of PSF in (18), letting $\hat{f} = F(f)$, the convolution operator can be written as $f \otimes h = F^* \Lambda F h$, where Λ is a diagonal matrix with diagonal entries $\hat{f}$. Let $M = F^* \Lambda F$, therefore :

$$h = \arg\min_{z,h} \|z\|_1 + \frac{\mu}{2\lambda_1}\|Mh - g\|_2^2 + < y, z - Dh > + \eta_r \|Dh - z\|_2^2. \tag{19}$$

To apply alternating direction method, we have the following algorithm [31] :

Algorithm 3

FIGURE 1. Original images : Cameraman, Peppers, Shepp-Logan, Satellite (from left to right).

for $k = 1, 2, 3, ...$ **do**

1. $h^{k+1} = \arg\min_h \frac{\mu}{2\lambda_1}\|Mh - g\|_2^2 - < y, z - Dh > +\eta_r\|z - Dh\|^2$,
2. $z^{k+1} = \arg\min_z \|z\|_1 - < y, z - Dh^{k+1} > +\eta_r\|z - Dh^{k+1}\|^2$,
3. $y^{k+1} = y^k - \eta_r(z^{k+1} - Dh^{k+1})$,
4. $\eta_r = \begin{cases} \delta\eta_r, & \text{if } \|z^{k+1} - Dh^{k+1}\|_2 \geq \xi\|z^k - Dh^k\|_2 \\ \eta_r, & \text{otherwise.} \end{cases}$

end

To solve step 1, by considering normal equations, we have:

$$(\mu M^*M + \eta_r D^*D)h = \mu M^*g + \eta_r D^*z - D^*y. \tag{20}$$

Using the Fourier transform, Eq. (20) will have the following solution:

$$h = F^*\left[\frac{F(\mu M^*g + \eta_r D^*z - D^*y)}{\mu|FM|^2 + \eta_r(|FD_x|^2 + |FD_y|^2)}\right]. \tag{21}$$

In step 2, the explicit formulas for z is:

$$z = \text{shrink}(Dh + \frac{1}{\eta_r}y, 1/\eta_r).$$

b. f-Subproblem: We use Fast alternative direction method for restoring original image ,f, similar to section 3.

B. blind deconvolution by SH-SH regularization

In the second model, shearlet transform is used as regularization term of an image and PSF as:

$$\min_{f,h} \ \frac{\mu}{2}\|f \otimes h - g\|_2^2 + \tau_1 \sum_{i=1}^{N} \|SH_i(h)\|_1 + \tau_2 \sum_{i=1}^{N} \|SH_i(f)\|_1. \tag{22}$$

To solve this problem, we propose the following algorithm :

Algorithm 4.

Input: an initial image f, an initial blur h and an observed image g

1.**for** $k = 1, 2, 3, ...$ **do**

2. Solve for h^k:

$$h^k = \arg\min_h \ \frac{\mu}{2}\|f^{k-1} \otimes h - g\|_2^2 + \tau_1 \sum_{i=1}^{N} \|SH_i(h)\|_1, \tag{23}$$

3. Solve for f^k:

$$f^k = \arg\min_f \ \frac{\mu}{2}\|f \otimes h^k - g\|_2^2 + \tau_2 \sum_{i=1}^{N} \|SH_i(f)\|_1, \tag{24}$$

end

In order to obtain the solution in steps 2 and 3, we used ADMM method. In next section, we will show the performance of the proposed blind deconvolution algorithms.

FIGURE 2. row 1: Images degraded by a Gaussian PSF with variance 5, BSNR=30, row 2: Restored images by SH-SH BD, row 3: Restored images by SH-TV BD, row 4: Restored images by Non-blind deconvolution Fast ADDM.

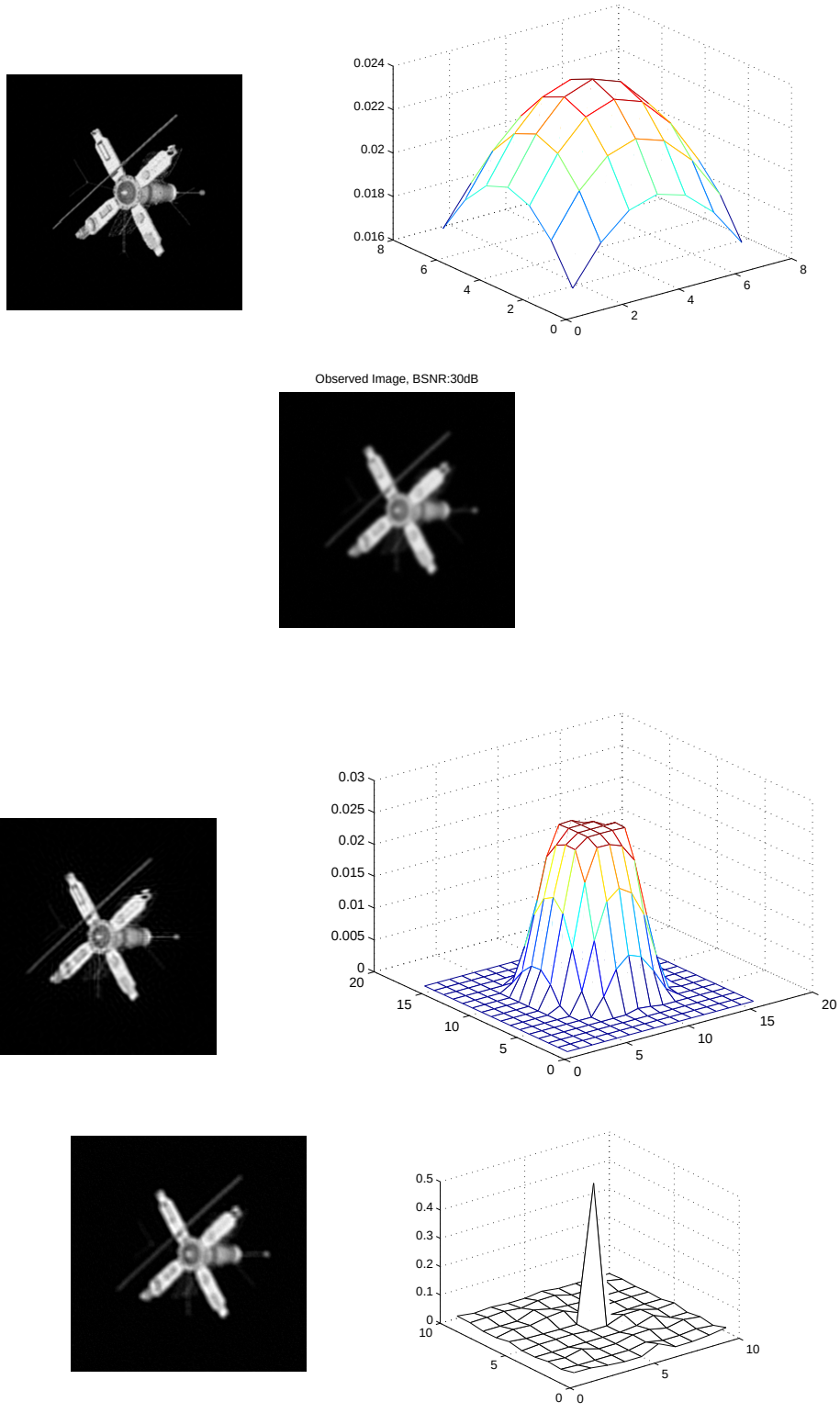

FIGURE 3. row 1: Original image and original PSF, row 2: Image degraded by a Gaussian(7,5), BSNR=30, row 3: Restored image and PSF by SH-TV BD method, row 4: Restored image and PSF by SH-SH BD method.

5. Numerical Results

Here, we use the presented methods (Shearlet-Total variation blind deconvolution (SH-TV BD) and Shearlet-Shearlet blind deconvolution (SH-SH BD)) for restoring degraded image and PSF for some images with different kinds of PSFs and noise levels. We use peak signal to noise ratio (PSNR) and improvement in signal-to-noise ratio (ISNR) to measure the quality of the restored images. Also blurred signal-to-noise ratio (BSNR) is used to measure the noise contained in observed image, which are defined as follows:

$$\text{PSNR} = 20\log_{10}\frac{255}{\|f-u\|_2},\ \text{ISNR} = 20\log_{10}\frac{\|f-g\|_2}{\|f-u\|_2},\ \text{BSNR} = 20\log_{10}\frac{\|g\|_2}{\|n\|_2},$$

where f, g, u and n, are the original image, observed image, recovered image and the noise vector respectively. In all tests, we use the observed image as an initial image and the delta function as an initial PSF. Table 1 displays the results for Peppers, Cameraman, Shepp-Logan and Satellite images presented in Figure 1. Images degraded by Gaussian PSFs with variance 5 of size 7 and Gaussian noise with BSNR=30dB. For all images in SH-TV blind deconvolution, parameter λ_1 is varying from 10^6 to 10^8 and $\lambda_2 = 0.2$. Table 1 shows that the results of the presented blind deconvolution methods (specially SH-TV method), is comparable to that of the nonblind deconvolution one. Figure 2 shows the obtained results using shearlets-total variation blind deconvolution, shearlet-shearlet blind deconvolution and Fast ADMM deconvolution where PSF is known, for Peppers and Cameraman images.

Table 1. Comparison result in PSNR, blurred image by Gaussian(7,5), BSNR=30 dB.

blured	Sh-TV BD	SH-SH BD	non-blind [32]
Peppers	24.73	23.36	27.42
Cameraman	24.10	22.11	26.74
Shepp-Logan	29.71	24.79	34.37
Satellite	30.28	27.23	31.02

We also compare the Shearlet-Total variation blind deconvolution method with the blind deconvolution algorithms in [21, 22]. Obtained results are in Tables 2 and 3. In [21] authors used total variation function as the image and the point spread function priors. In [22] authors used the total variation function as the image prior and a simultaneous autoregressive (SAR) model as the PSF prior. In these tests, the Cameraman and Shep-Logan images, degraded by Gaussian PSFs with variance 5 of size 10 and Gaussian noises with BSNR=40dB and 20dB. The parameter λ_1 is varying from 10^6 to 10^8 and $\lambda_2 = 0.2$. It can be observed that for the Gaussian PSF, the SH-TV blind deconvolution method outperforms the other three methods. Figure 3, shows the results of presented methods on Satellite image degraded by kernel gaussian(7,5) and BSNR=30.

Table 2. Comparison in ISNR on Gaussian PSF with variance 5.

Cameraman	SH-TV BD	TV1[22]	TV2[22]	Method[21]
BSNR=40	1.58	1.66	2.49	1.32
BSNR=20	1.48	1.43	-42.54	1.17

Table 3. Comparison in ISNR on Gaussian PSF with variance 5 .

Shep-Logan	SH-TV BD	TV1[22]	TV2[22]
BSNR=40	4.18	2.05	3.79
BSNR=20	4.09	2.09	-26.00

6. Conclusions

In this paper we presented two blind deconvolution methods: SH-TV method and SH-SH method. By using of shearlet transform, we are able to restoring more details of images with complex tissues. Obtained results show the efficiency of the presented methods for image recovering in minimization problems. Also our results for blind deconvolution, is comparable to those of the nonblind deconvolution.

References

[1] Patel, V. M., Easley, G. R. and Healy, D. M.,(2009) Shearlet-Based Deconvolution, IEEE Trans. Image Process, 18(12) pp. 2673-2685.
[2] Campisi, P. and Egiazarian, K. ,(2007) Blind Image Deconvolution: Theory and Applications. Boca Raton, FL: CRC.
[3] Nakagaki, R. and Katsaggelos, A. K., (2003) , A VQ-based blind image restoration algorithm, IEEE Trans. Image Process., 12(9) pp. 1044-1053.
[4] Panchapakesan, K. Sheppard, D. G. Marcellin, M. W. and Hunt, B.R. (2001), Blur identification from vector quantizer encoder distortion, IEEE Trans. Image Process., 10(3) pp. 465-470.
[5] Kundur, D. and Hatzinakos, D.(1998) , A novel blind deconvolution scheme for image restoration using recursive filtering, IEEE Trans. Signal Process., 46(2) pp. 375-390.
[6] Ng, M. Plemmons, R. and Qiao, S. (2000), Regularization of RIF blind image deconvolution, IEEE Trans. Image Process., 9(6) pp. 1130-1134.
[7] Ong, C. and Chambers, J.(1999), An enhanced NAS-RIF algorithm for blind image deconvolution, IEEE Trans. Image Process., 8(7) pp. 982-992.
[8] Stockham,T. G. Cannon, T. M. and Ingebretsen, R. B., (1975), Blind deconvolution through digital signal processing, Proc. IEEE, 64(4) pp. 678-692.
[9] Cannon, M.,(1976), Blind deconvolution of spatially invariant image blurs with phase,IEEE Trans. Acoust., Speech, Signal Process., 24(1) pp. 58-63.
[10] Lane, R. G. and Bates, R. H. T., (1987) , Automatic multidimensional deconvolution, J. Opt. Soc. Amer. A, 4(1) pp. 180-188.
[11] Katsaggelos, A. and Lay, K., (1989), A. Katsaggelos and K. Lay, Simultaneous blur identification and image restoration using the EM algorithm, in Proc. SPIE Conf, Visual Commun. Image Process. IV, 1199 pp. 1474-1485.
[12] Lagendijk, R. Tekalp, A. and Bidmond, J., (1990) Maximum likelihood image and blur identification: A unifying approach, Opt. Eng., 29 pp. 422-435.
[13] Liao, H. and Ng, M. K., (2011), Blind deconvolution using generalized cross-validation approach to regularization parameter estimation, IEEE, Transactions on Image Processing, 20(3) pp. 670-680.
[14] Likas, A. C. and Galatsanos, N. P., (2004), A variational approach for Bayesian blind image deconvolution, IEEE Trans. Signal Process., 52(8) pp. 2222-2233.
[15] Molina, R. Mateos, J. and Katsaggelos, A. K., (2006), Blind deconvolution using a variational approach to parameter, image, and blur estimation, IEEE Trans. Image Process., 15(12) pp. 3715-3727.
[16] Tzikas, D. Likas, A. and Galatsanos, N., (2009) Variational Bayesian sparse kernel-based blind image deconvolution with student's-t priors, IEEE Trans. Image Process., 18(4) pp. 753-764.
[17] Reeves, S. and Mersereau, R., (1992) Blur identification by the method of generalized cross-validation, IEEE Trans. Image Process., 1(3) pp. 301-311.
[18] Miskin, J.W. and MacKay, D. J. C., (2000) Ensemble learning for blind image separation and deconvolution, in Advances in Independent Component Analysis, M. Girolami, Ed. New York: Springer-Verlag.
[19] Adami, K. Z., (2003), Variational methods in Bayesian deconvolution, PHYSTAT2003, SLAC, Stanford, California, pp. 8-11.
[20] You, Y. and Kaveh, M., (1996)), A regularization approach to joint blur identification and image restoration, IEEE Trans. Image Process, 5(3) pp. 416-427.

[21] Chan, T. F. and Wong, C. K., (1998) Total variation blind deconvolution, IEEE Trans. Image Process., 7(3) pp. 370-375.
[22] Babacan, S. D. Molina, R. and Katsaggelos, A. K., (2009), Variational Bayesian blind deconvolution using a total variation prior, IEEE Trans. Image Process., 18(1) pp. 12-26.
[23] You, Y. and Kaveh, M., (1999), Blind image restoration by anisotropic regularization, IEEE Trans. Image Process, 8(3) pp. 396-407.
[24] Huang, Y. and Ng, M. (2008), Lipschitz and total-variational regularization for blind deconvolution, Commun. Comput. Phys., 4 pp. 195-206.
[25] Kundur, D. and Hatzinakos, D. , (1996), Blind image deconvolution, IEEE Signal Process. Mag., 13(3) pp. 43-64.
[26] Rudin, L. Osher, S. and Fatemi, E., (1992), Nonlinear total variation based noise removal algorithms, Physica D, 60 pp. 259-268.
[27] Goldstein, T. O'Donoghue, B. Setzer, S. and Baraniuk, R., (2014), Fast Alternating Direction Optimization Methods, SIAM J. Imaging Sciences, 7(3) pp. 1588-1623.
[28] *Kutyniok, G. and D. Labate, D.*, (2009), Resolution of the wavefront set using continuous shearlets, Trans. Am. Math. Soc., 361 pp. 271-2754.
[29] Guo, W. Qin, J. and Yin, W., (2014), A New Detail-Preserving Regularization Scheme, SIAM J. Imaging Sciences, 7(2) pp. 1309-1334.
[30] Hauser, S., (2012) Fast Finite Shearlet Transform, preprint, arXiv:1202.1773.
[31] Chan, S. H. Khoshabeh, R. Gibson, K. B. Gill,P. E. and Nguyen, T. Q., (2011), An Augmented Lagrangian Method for Total Variation Video Restoration,IEEE Trans. Image Process., 20(11) pp. 3097-3111.
[32] He C., Hu, C. and Zhang, W., (2014), Adaptive shearlet-regularized image deblurring via alternating direction method, Multimedia and Expo (ICME), IEEE International Conference.

Zohre Mousavi Rizi was born 1982 in Iran. She received the B.Sc degree in Applied mathematics in 2004 and the M.Sc degree in Pure Mathematics in 2006, both from the University of Yazd in Iran and currently pursuing the Doctor degree in Applied mathematics at Esfahan Technology university in Iran . Her research interests include: Image processing, shearlet and minimization methods .

Reza Mokhtari received his Ph.D. in Applied Mathematics (Numerical Analysis) in 2005 at Iran University of Science and Technology in Tehran, Iran. Since 2005 he has been working at the Department of Mathematical Sciences of Isfahan University of Technology, Isfahan, Iran. He is currently an associate professor and his main research interest is numerical solution of differential equations.

Mehrdad Lakestani is a Professor at Department of Applied Mathematics in University of Tabriz. He was born in Khoy, West Azarbayjan, Iran, in 1976. He started his job as an academic staff at University of Tabriz, Iran, since 2005. He received his Ph.D. degree at Amirkabir University of Technology (Tehran Polytechnic), Tehran, Iran in 2005. His interests are mainly numerical analysis, optimal control, wavelets and image processing.